



Published in final edited form as:

Lancet Oncol. 2018 August ; 19(8): 1040–1050. doi:10.1016/S1470-2045(18)30322-X.

Convection-enhanced delivery for diffuse intrinsic pontine glioma: a single-centre, dose-escalation, phase 1 trial

Mark M Souweidane, Kim Kramer, Neeta Pandit-Taskar, Zhiping Zhou, Sofia Haque, Pat Zanzonico, Jorge A Carrasquillo, Serge K Lyashchenko, Sunitha B Thakur, Maria Donzelli, Ryan S Turner, Jason S Lewis, Nai-Kong V Cheung, Steven M Larson, Ira J Dunkel (Prof M M Souweidane MD), **Department of Pediatrics** (Prof K Kramer MD, Z Zhou PhD, M Donzelli MSN, R S Turner BS, Prof N-K V Cheung MD, Prof I J Dunkel MD), **Department of Radiology, Molecular Imaging and Therapy (Nuclear Medicine) Service** (Prof N Pandit-Taskar MD, Prof J A Carrasquillo MD, Prof S M Larson MD), **Department of Radiology** (S Haque MD, P Zanzonico PhD, S K Lyashchenko PharmD, S B Thakur PhD, Prof J S Lewis PhD), **Department of Medical Physics** (P Zanzonico, S B Thakur), **Radiochemistry & Molecular Imaging Probes Facility** (S K Lyashchenko, Prof J S Lewis), **and Center for Targeted Radioimmunotherapy and Theranostics, Ludwig Center for Cancer Immunotherapy** (Prof N Pandit-Taskar, Prof J A Carrasquillo, Prof S M Larson), **Memorial Sloan Kettering Cancer Center, New York, NY, USA; Molecular Pharmacology Program, Sloan Kettering Institute, New York, NY, USA** (Prof S M Larson); **Department of Neurological Surgery** (Prof M M Souweidane, Z Zhou), **Department of Pediatrics** (Prof M M Souweidane, Prof K Kramer, Prof I J Dunkel), **and Department of Radiology** (Prof N Pandit-Taskar, S Haque, Prof J A Carrasquillo, S K Lyashchenko, Prof J S Lewis, Prof S M Larson), **Weill Medical College of Cornell University, New York, USA; and Pharmacology Program, Weill Cornell Graduate School of Medical Sciences, Cornell University, New York, NY, USA** (Prof J S Lewis)

Summary

Correspondence to: Prof Mark M Souweidane, Department of Neurological Surgery, Weill Medical College of Cornell University, New York, NY 10065, USA, mmsouwei@med.cornell.edu.

Contributors

MMS, ZZ, IJD, KK, and N-KVC contributed to the study conception and MMS, ZZ, IJD, NP-T, KK, PZ, JAC, SKL, JSL, SH, SBT, N-KVC, and SML contributed to the study design. MMS, NP-T, KK, IJD, SH, PZ, ZZ, JAC, SKL, JSL, SBT, MD, and RST acquired the data. Data management was done by RST and MD. MMS, ZZ, NP-T, PZ, SH, SBT, RST, and MD analysed the data. MMS, IJD, KK, NP-T, SH, ZZ, PZ, and JAC interpreted the results. MMS, ZZ, NP-T, IJD, KK, PZ, SKL, JSL, and N-KVC drafted the manuscript with critical revision from MMS, ZZ, IJD, NP-T, JAC, KK, SKL, and JSL. All authors gave approval for the manuscript to be submitted.

Declaration of interests

The antibody 8H9 was licensed by MSKCC to Y-mAbs Therapeutics. N-KVC reports financial interest in and research support from Y-mAbs Therapeutics, a grant from Abpro-Labs, personal fees and other support from Abpro-Labs and Eureka Therapeutics; N-KVC was also named an inventor in the patents filed by MSKCC (US issued patents 6451995, 7666424, and 9315585 licensed to Y-mAbs Therapeutics; 7507724 and 7704973 licensed to Biotech Pharmacon; 6939948, 9040669, and 9453075; three pending patents licensed to Y-mAbs Therapeutics; one pending patent licensed to Abpro-Labs; and nine other pending patents).

SML reports personal fees and other support from Janssen, Progenics, and Merck; grants from Regeneron; other support from ImaginAB, Cynvec, Elucida Theranostic, and Voreyda Theranostic. IJD reports non-financial support from Apexigen; personal fees from Bayer, Celgene, Eisai, Ipsen, and Pfizer; grants and personal fees from Bristol-Myers Squibb; and grants from Novartis and Genentech. JAC reports other support from Y-mAbs Therapeutics. KK reports other support from Y-mAbs Therapeutics. MMS reports other support from Aesculap.

All other authors declare no competing interests.

Background—Diffuse intrinsic pontine glioma is one of the deadliest central nervous system tumours of childhood, with a median overall survival of less than 12 months. Convection-enhanced delivery has been proposed as a means to efficiently deliver therapeutic agents directly into the brainstem while minimising systemic exposure and associated toxic effects. We did this study to evaluate the safety of convection-enhanced delivery of a radioimmunotherapy agent targeting the glioma-associated B7-H3 antigen in children with diffuse intrinsic pontine glioma.

Methods—We did a phase 1, single-arm, single-centre, dose-escalation study at the Memorial Sloan Kettering Cancer Center (New York, NY, USA). Eligible patients were aged 3–21 years and had diffuse intrinsic pontine glioma as diagnosed by consensus of a multidisciplinary paediatric neuro-oncology team; a Lansky (patients <16 years of age) or Karnofsky (patients ≥16 years) performance score of at least 50 at study entry; a minimum weight of 8 kg; and had completed external beam radiation therapy (54.0–59.4 Gy at 1.8 Gy per fraction over 30–33 fractions) at least 4 weeks but no more than 14 weeks before enrolment. Seven dose-escalation cohorts were planned based on standard 3 + 3 rules: patients received a single infusion of 9.25, 18.5, 27.75, 37, 92.5, 120.25, or 148 MBq, respectively, at a concentration of about 37 MBq/mL by convection-enhanced delivery of the radiolabelled antibody [¹²⁴I]-8H9. The primary endpoint was identification of the maximum tolerated dose. The analysis of the primary endpoint was done in the per-protocol population (patients who received the full planned dose of treatment), and all patients who received any dose of study treatment were included in the safety analysis. This study is registered with [ClinicalTrials.gov](https://clinicaltrials.gov), number [NCT01502917](https://clinicaltrials.gov/ct2/show/study/NCT01502917), and is ongoing with an expanded cohort.

Findings—From April 5, 2012, to Oct 8, 2016, 28 children were enrolled and treated in the trial, of whom 25 were evaluable for the primary endpoint. The maximum tolerated dose was not reached as no dose-limiting toxicities were observed. One (4%) of 28 patients had treatment-related transient grade 3 hemiparesis and one (4%) had grade 3 skin infection. No treatment-related grade 4 adverse events or deaths occurred. Estimated volumes of distribution (V_d) were linearly dependent on volumes of infusion (V_i) and ranged from 1.5 to 20.1 cm³, with a mean V_d/V_i ratio of 3.4 (SD 1.2). The mean lesion absorbed dose was 0.39 Gy/MBq ¹²⁴I (SD 0.20). Systemic exposure was negligible, with an average lesion-to-whole body ratio of radiation absorbed dose higher than 1200.

Interpretation—Convection-enhanced delivery in the brainstem of children with diffuse intrinsic pontine glioma who have previously received radiation therapy seems to be a rational and safe therapeutic strategy. PET-based dosimetry of the radiolabelled antibody [¹²⁴I]-8H9 validated the principle of using convection-enhanced delivery in the brain to achieve high intra-lesional dosing with negligible systemic exposure. This therapeutic strategy warrants further development for children with diffuse intrinsic pontine glioma.

Funding—National Institutes of Health, The Dana Foundation, The Cure Starts Now, Solving Kids' Cancer, The Lyla Nsouli Foundation, Cookies for Kids' Cancer, The Cristian Rivera Foundation, Battle for a Cure, Cole Foundation, Meryl & Charles Witmer Charitable Foundation, Tuesdays with Mitch Charitable Foundation, and Memorial Sloan Kettering Cancer Center.

Introduction

Diffuse intrinsic pontine glioma is the most common childhood brainstem malignancy with a median overall survival of less than 12 months.^{1,2} The poor track record of systemic chemotherapy, including investigational therapies, and the recognition of an intact blood-brain barrier³ in this disease support the use of direct drug delivery as a new therapeutic strategy.

Convection-enhanced delivery (CED) is a form of direct delivery that bypasses the blood-brain barrier, producing high local drug concentrations with limited systemic exposure.⁴ We postulated that this strategy can produce sufficient tumour coverage and therapeutic drug concentrations for treatment of diffuse intrinsic pontine glioma. Given the anatomical complexity and critical functions of the brainstem, convection-enhanced delivery might seem to be an implausible therapeutic means for this disease, but preclinical research has showed good safety and feasibility.⁵ The earliest attempts using convection-enhanced delivery have been highly varied with respect to agent, infusate volume, infusion rate, cannula design, surgical approach, and stage of the disease course. As a result, categorical assessments of this strategy have not been possible in children with diffuse intrinsic pontine glioma.

The monoclonal antibody 8H9 is a murine antibody that binds the surface antigen B7-H3,⁶ an immune modulator of natural killer and T cells that is overexpressed in the majority of high-grade gliomas,⁷ including diffuse intrinsic pontine glioma.⁸ The radioisotope ¹²⁴I imparts its energy through emitting positrons and gamma rays. Although ¹³¹I is the main iodine radioisotope used for therapeutic applications, the positrons emitted by ¹²⁴I also have sufficiently high energy and abundance and suitable penetrability for use in therapy for bulky lesions, with an average range in soft tissue of 1.15 mm.⁹ The emission of annihilation gamma rays allows for use of PET, and thus substantially higher spatial resolution and more accurate imaging-based activity quantitation and radiation dosimetry than is achievable with ¹³¹I, which is assessed using singlephoton emission CT. The use of ¹²⁴I as a theranostic radioisotope at clinically meaningful doses, a novel feature of this study, is made possible by the local delivery of [¹²⁴I]-8H9. It has previously been shown that [¹²⁵I]-8H9 does not substantially internalise when bound to its target antigen B7-H3 so a high rate of dehalogenation would not be expected.¹⁰ We did a phase 1 clinical trial to assess the safety of convection-enhanced delivery of [¹²⁴I]-8H9 radioimmunotherapy in patients with diffuse intrinsic pontine glioma.

Methods

Study design and participants

This investigator-initiated, single-arm, single-centre, phase 1 clinical trial followed a standard 3 + 3 dose- escalation design.¹¹

When a query was received from a family or referring oncologist, the patient was screened via telephone by the study coordinator. Clinical records and imaging studies were reviewed and presented at a multidisciplinary conference. If the patient was deemed preliminarily

eligible, then the patient was invited for onsite evaluation. Eligible patients were aged 3–21 years and had diffuse intrinsic pontine glioma as diagnosed by consensus of a multidisciplinary paediatric neuro-oncology team based on clinical evidence and MRI at presentation (tissue diagnosis was not required for study entry); had completed external beam radiation therapy (54.0–59.4 Gy at 1.8 Gy per fraction over 30–33 fractions) at least 4 weeks but no more than 14 weeks before enrolment; were in adequate general condition, with a Lansky (patients <16 years of age) or Karnofsky (patients ≥16 years of age) performance score of at least 50 at study entry; and had a minimum weight of 8 kg. Patients were excluded if there was any evidence of clinical or radiographic progression following external beam radiation therapy, dissemination, untreated symptomatic hydrocephalus, or inadequate general condition (appendix p 1). Patients who had received chemotherapy were permitted if they had undergone a washout period of at least 30 days. Patients on corticosteroid therapy were not excluded.

The study was approved by the Memorial Sloan Kettering Cancer Center (MSKCC) institutional review board and the US Food and Drug Administration. Study patients, their parents or legal guardians provided written informed consent to participate.

Procedures

As per the 3 + 3 design, dose escalation of [¹²⁴I]-8H9 was started, and after completion of each dose level, an interim analysis was performed to evaluate toxicities and PET data for clearance and dosimetry. Initially, four dose cohorts of three to six patients each were planned to receive escalating doses of [¹²⁴I]-8H9 administered in a maximum volume of 1 mL (cohorts 1–4; figure 1), however, absence of treatment-related adverse events in the patients enrolled in these first four cohorts led to a protocol amendment on July 1, 2014, that allowed administration volumes to be escalated with corresponding activities in the following cohorts (5–7). After the protocol amendment, because the dose increase between cohorts 4 and 5 was higher than that between previous dose levels, two new fallback levels were added at this stage (appendix pp 1, 2). The amended protocol included seven dose levels in total, for a single infusion of 9.25, 18.5, 27.75, 37, 92.5, 120.25, and 148 MBq, respectively, at a concentration of about 37 MBq/mL (figure 1; appendix p 3). Specific activity (activity per unit mass of antibody, aiming for 74 MBq/mg antibody) and activity concentration (activity per unit volume, aiming for 37 MBq/mL) were held constant, therefore activity (amount of the radioactive source), infusion volume, and mass of antibody were simultaneously escalated. The study is ongoing, with an expanded cohort currently at dose level 7.2.

8H9 was produced as previously described,⁷ and radiolabelled with ¹²⁴I at the MSKCC Radiochemistry and Molecular Imaging Probes Core Facility using the Iodogen method in compliance with investigational new drug number BB-IND 9351. The mean specific activity of the radiolabelled antibody was 72.15 MBq/mg (range 65.12–77.7) and the mean radioactive concentration was 36.63 MBq/mL (29.6–39.59).

To block thyroid uptake of ¹²⁴I released from the administered radiolabelled antibody, saturated potassium iodide oral solution (seven drops daily) and liothyronine (25 µg/day if weight <25 kg, 50 µg/day if weight ≥25 kg) were started 5 days before the infusion of

[¹²⁴I]-8H9 and continued for 2 weeks after the procedure. Dexamethasone was continued for those patients on steroids at the time of study entry and at the discretion of the principal investigator.

Stereotactic placement of the infusion catheter was done via a supratentorial (transfrontal) route with a fully MR-compatible navigational interface (ClearPoint, MRI Interventions, Irvine, CA, USA) to target the central region of the tumour (appendix p 4). In the first 16 patients (cohorts 1–4 and the first two patients on cohort 5), a SmartFlow cannula (MRI Interventions, Irvine, CA, USA) was used and the infusion was administered with the patient under general anaesthesia. In the remaining 12 patients (the last patient recruited to cohort 5 and all patients on cohorts 6–7), a SmartFlow Flex catheter (Brainlab AG, Munich, Germany) was used with the infusion being done with the patient awake in the paediatric intensive care unit. The change to the use of the paediatric intensive care unit was to allow for longer infusions where the patients were kept awake for neurological examination. For infusions done in the paediatric intensive care unit, patients were intravenously sedated at the discretion of the intensive care physician.

The infusion set-up was primed with [¹²⁴I]-8H9 followed by the actual infusion of the prescribed activity by use of a micro-infusion pump (Harvard Apparatus, Holliston, MA, USA). Infusions were done using an escalating flow rate plan with 10-min intervals until the maximum rate was achieved (0.5 µL/min, 1.0 µL/min, 2.0 µL/min, 5.0 µL/min, and 7.5 µL/min.). The catheter was removed shortly after the completion of the infusion (<1 h).

MRI was used to monitor subclinical adverse events, surgical accuracy, distribution, and for exploratory therapeutic response analysis. All patients underwent MRI of the brain within 14 days before therapy, and then on day 1 and day 30 (± 4 days) post-infusion (appendix p 2). The last patient on cohort 2, patients treated on cohorts 3–4, and the first two patients on cohort 5 underwent additional intraoperative MR scans at 20–60 min intervals. Volume of distribution (Vd) was measured from T₂-weighted images (appendix p 5) using the seed-growing segmentation method in iPhan Flow version 3.0 (Brainlab).

Serial PET/CT scans (a minimum of three and a maximum of five) were done for all patients to assess localisation of [¹²⁴I]-8H9 in the brain and to obtain quantitative data to assess radiation absorbed dose (appendix p 2). PET/CT scans were done within 1–6 h, and then at 48 h (±24 h), 96 h (±24 h), and 7 days (±1 day) after completion of infusion, with up to two optional scans between days 7 and 14. Radiation dosimetry was done using standard methods with medical internal radionuclide dosimetry. Using region of interest analysis, standardised uptake values within the whole body and the lesion were generated at all timepoints of the PET imaging, and activity concentration (in kBq/g of tissue or kBq/g body mass) was calculated. The total cumulative activity (in kBq-h), which is equivalent to the area under the ¹²⁴I time-activity curve, was calculated. Radiation absorbed doses to the whole body and to the lesion were then calculated using the *OLINDA* radionuclide dosimetry program, version 1.0¹² (appendix p 2).

Blood was sampled for human anti-mouse antibody preoperatively and at days 14 and 30 postoperatively. Blood sampling for radioisotope clearance was done concurrently with

PET/CT imaging. Patients remained in hospital for observation for the first 4 days and then had weekly outpatient visits until 30 days, at which point routine primary oncologist visits were resumed.

Adverse events were classified in accordance with the National Cancer Institute Common Terminology Criteria for Adverse Events (CTCAE) version 4. Adverse events were assessed several times a day while the patient was in hospital and at the weekly outpatient visits thereafter. Dose interruptions were planned to occur if there was suspected or confirmed neurological injury or intracranial haemorrhage or malfunction of the infusion circuit. Patients were to be removed from the study in the event of non-compliance with treatment plan, withdrawal of consent for participation, progression of disease before intervention, or death.

Outcomes

The primary endpoint was identification of the maximum tolerated dose of [¹²⁴I]-8H9 administered by convection-enhanced delivery, defined as the dose level below the one where dose-limiting toxicities had occurred in two patients. Within the first 30 days after [¹²⁴I]-8H9 delivery, grade 3 nervous system adverse events that did not improve or resolve spontaneously or with dexamethasone administration within 1 week, and any grade 4 or 5 adverse events, were deemed to be dose-limiting toxicities.

Secondary endpoints included estimation of absorbed doses (the energy of radiation absorbed per unit mass of tissue) and volumes of distribution (the volume of tissue where the infusate distributes to) of [¹²⁴I]-8H9, assessment of the toxicity profile associated with [¹²⁴I]-8H9 administered via convection-enhanced delivery to the brainstem, description of overall survival (the time interval between diagnosis and death from any cause). Performance status was explored as an indicator of quality of life. Advanced neuroimaging and magnetic resonance spectroscopy were used for exploratory therapeutic response analysis and will be reported separately.

Statistical analysis

We hypothesised that convection-enhanced delivery of [¹²⁴I]-8H9 in patients with diffuse intrinsic pontine glioma would be safe if performed with protocol-defined parameters. The absence of grade 4 or 5 adverse events and a low frequency of grade 3 events would be regarded as evidence of the safety of this intervention. We estimated to enrol up to 42 patients on seven dose levels based on standard 3 + 3 dose escalation rules.

The analyses for primary and secondary endpoints were per protocol—ie, all patients who received one full dose of study treatment were considered to be evaluable. Patients who had received less than the prescribed dose due to malfunction of the infusion circuit or as detected with PET dosimetry were excluded from these analyses. All patients were included in procedure-related safety analysis.

Overall survival was assessed with the Kaplan-Meier method. The CI for median survival was calculated via the Brookmeyer and Crowley method,¹³ which is based on inverting a sign test. Pointwise CIs of survival probability were calculated using the log transform of the

estimated standard deviation (square root of the Greenwood formula¹⁴). Scores for performance status were summarised with descriptive statistics. For continuous data, averages are expressed as mean (SD) unless stated otherwise. Statistical tests were done and graphs were plotted in R version 3.4.1–3.4.4.

The study was overseen by the MSKCC data and safety monitoring committee approved by the National Cancer Institute. This study is registered with [NCT01502917](#), and is ongoing with an expanded cohort.

Role of the funding source

The funders reviewed the design during funding applications, but otherwise had no role in study design, data collection, data analysis, data interpretation, or writing of the report. Y-mAbs Therapeutics, the current rights holder of 8H9 (MSKCC licensed 8H9 to Y-mAbs in August 2015), reviewed the manuscript before submission. The corresponding author had full access to all the data in the study and had final responsibility for the decision to submit for publication.

Results

475 patients were preliminarily screened via phone call or email; most were identified upfront as being ineligible because of their age, disease progression, being more than 14 weeks beyond radiation therapy, or having low performance status. From April 5, 2012, to Oct 8, 2016, 28 patients were enrolled in the trial (table 1), of whom 25 (89%) were deemed evaluable for the primary and secondary endpoints; three patients were deemed unevaluable because of incomplete planned dose administration (one had excessive egress into the subarachnoid space and two had circuit disconnections during administration), but were included in the assessment of procedure-related adverse events (figure 1). The volumes of infused [¹²⁴I]-8H9 ranged from 0.24 mL to 4.4 mL, and infusion time ranged from 1.18 h to 16.6 h (figure 1; appendix p 3).

The maximum-tolerated dose was not reached and no dose-limiting toxicities occurred. A recommended phase 2 dose was not established. [¹²⁴I]-8H9 administered by convection-enhanced delivery using the defined techniques and parameters was well tolerated. No patients required dose reductions and no patients discontinued participation because of drug-related toxicity. No treatment-related deaths occurred.

As of March 16, 2018 (interim analysis cutoff date), 25 patients (of whom 22 were among those evaluable for the primary outcome) had died: all deaths were the result of disease progression. For the three surviving patients, median follow-up was 36.1 months. Table 2 shows all-cause adverse events. The most common adverse events related to the study intervention as per investigator assessments were transient grade 1 or 2 headache (11 [39%] of 28 patients), pain (seven [25%] patients), mild motor weakness (eg, hemiparesis; five [18%] patients), and cranial neuropathy (eight [29%]); one (4%) patient experienced grade 3 hemiparesis and one (4%) patient had grade 3 skin infection (appendix p 7). Most motor weakness symptoms resolved spontaneously or with dexamethasone, usually within the first 1–4 days after infusion. Biochemical abnormalities were infrequent; transient grade 1 or 2

elevations of alanine aminotransferase and aspartate aminotransferase were noted in two (7%) patients. All catheters were adequately positioned at the planned target site in the pontine lesion on the first attempt. All patients remained negative for human anti-mouse antibody during the 30-day mandated observation period.

MR imaging on day 1 and day 30 did not reveal any appreciable haemorrhage in any patients. In five (18%) of 28 patients (one at cohort 2, one at cohort 3, one at cohort 6, and two at cohort 7), MRI on day 1 showed small foci (1–3 mm) of blood signals at the cannula tip or for a short length along the cannula tract on T2*-Weighted ANgiography (SWAN) images, but not on other sequences. All of these blood signals remained stable or reduced by the day 30 scans. In five (18%) of 28 patients (one in cohort 5, one in cohort 6, and three in cohort 7), scans on day 30 showed an increase in the areas of necrosis of the tumour of 2–5 mm in one or two dimensions compared with baseline. New or increasing contrast enhancement was seen frequently but with variable temporal patterns (images not shown). New enhancement was mostly limited to the injection site and catheter path and usually fluctuated over the 30-day evaluation period. There was no appreciable new contrast enhancement at sites unrelated to the infusion.

Estimated volumes of distribution (Vd) were linearly dependent on volumes of infusion (Vi) and ranged from 1.5 cm³ to 20.1 cm³, with a mean Vd/Vi ratio of 3.4 (SD 1.2). Mean Vd was 1.8 cm³ (SD 0.3) for cohort 3, 2.8 cm³ (0.3) for cohort 4, 6.0 cm³ (0.5) for cohort 5, 17.4 cm³ (4.8) for cohort 6, and 15.8 cm³ (9.0) for cohort 7; mean Vd/Vi ratios was 2.5 (0.5), 2.7 (0.3), 2.3 (0.2), 5.0 (1.5), and 3.7 (1.1), respectively. Patients on dose levels 1 and 2 were not scanned for Vd determination, except one patient (on dose level 2). The linear relationship between Vd and Vi was present within individual patients across serial timepoints ($r^2=0.9712$; appendix p 6), as well as for total Vd and Vi across patients ($r^2=0.7549$; figure 2).

PET scans showed that [¹²⁴I]-8H9 localised in the brainstem lesion immediately after the infusion and remained in the lesion up to day 14. Lesion clearance was biexponential, with mean clearance half-time of 36 h (SD 12) for the fast component and 59 h (69) for the slow component. By comparison, activities in the rest of the body were noted as being three orders lower than in the lesion and cleared steadily over time, with a mean half-time of 57.2 h (27.0). High-contrast intense concentration of activity was noted in the brainstem lesion (figure 3), with the average fraction of total activity in the body localised in the lesion being 61% (SD 22) on the first scans. The average total absorbed dose in the lesion was 26.94 Gy and the average per-MBq absorbed dose was 0.39 Gy/MBq (0.20). In general, the total absorbed doses of radiation increased with the total infused activity, with averages ranging from 14.48 Gy for cohort 1 to 24.42 Gy for cohort 7. By comparison, the average whole-body absorbed dose for all dose levels was 0.0336 Gy (0.0324). The lesion-to-whole-body absorbed dose ratio was 1285 (1019).

As of March 16, 2018, the median overall survival of the 25 evaluable patients was 15.3 months (IQR 11.4–17.2, 95% CI 14.7–22.5; figure 4A); three patients remained alive, with a median follow-up of 36–1 months (IQR 31.3–48.8). Median overall survival by dose level was 10.0 months (95% CI 6.6–not reached [NR]) at dose level 1, 10.6 months (9.4–NR) at

dose level 2, 16.8 months (15.3–NR) at dose level 3, 17.1 months (11.4–NR) at dose level 4, 15.3 months (11.2–NR) at dose level 5, 26.1 (22.9–NR) at dose level 6, and 15.0 months (13.2–NR) at dose level 7. Comparison of overall survival between dose levels with the Cox proportional hazards model resulted in a *p* value of 0.053 (figure 4B).

At the day 30 follow-up visits, 20 (71%) of 28 patients had Lansky or Karnofsky performance statuses that were unchanged from those at enrolment, three (11%) had higher scores, and five (18%) had lower scores. Full performance score data are shown in the appendix (p 8).

Discussion

To our knowledge, this study represents the first dose- escalation clinical trial of convection-enhanced delivery in children with diffuse intrinsic pontine glioma. In this study, up to 148 MBq [¹²⁴I]-8H9 in 4000 µL was infused, with infusion rates up to 7.5 µL/min. No dose-limiting toxicities occurred and therefore a maximum-tolerated dose was not reached. There were only two transient grade 3 treatment-related adverse events, no treatment-related grade 4 events, and no treatment-related deaths. An average lesion to whole-body absorbed dose ratio of more than 1200 was achieved. A single infusion volume of about 4000 µL resulted in a distribution volume that was similar to the average estimates of tumour volume after radiation therapy,¹⁵ suggesting that the material is distributed throughout the tumour, if perfectly aligned. These results showed the safety of this approach when tightly controlled parameters are used and provide validation of the fundamental principle of convection-enhanced delivery—that it is highly efficient in delivering drugs into the target area with negligible systemic exposure.

Nearly all previous reports on the use of convection-enhanced delivery in the brainstems of children with diffuse intrinsic pontine glioma have offered experimental treatment at the time of disease progression. This study was designed to enrol patients before disease progression, within 4–14 weeks after completing radiation therapy. We predicted that the disease burden during this time would be lowest, tolerance would be improved, and tumour coverage would be more probable. Intervention at this point in the disease continuum would also lessen the likelihood of disease progression during the 30-day observation period and hence reduce ambiguity in differentiating between treatment-associated adverse events and disease progression.

Few adverse events were attributable to the surgical procedure, despite the catheter trajectory intersecting major descending corticofugal pathways, including the internal capsule and the pyramidal tract. The relative lack of motor deficits was therefore an important finding on the tolerability of this approach and probably a testimony to the small scale of the catheter (outer diameter 1.8–2.1 mm). Only one patient had transient grade 3 hemiparesis as a result of the infusion. Post-infusion motor weakness did not seem to be dependent on dose or infusion rate and usually dissipated over several hours.

During the 30-day observation period, no major adverse events were attributed to the radioimmunotherapy. High radiation absorbed doses were delivered to the lesion with an

average of 0.39 Gy/MBq of ^{124}I administered, which was made possible by the retention of activity in the lesion for several days. For patients at cohort 7 (148 MBq), the absorbed dose was as high as 65 Gy. Considering that patients had received 54–59.4 Gy high-energy X-ray irradiation before study entry, the doses were considered to be well tolerated. The fact that the dose from the radioisotope is delivered over a period of days, with a dose rate lower than that of external beam radiation therapy (typically 2 Gy/min), probably allows for less acute radiation effects and time for the repair of non-targeted normal cells. Tolerance to high radiation absorbed doses delivered by a radioisotope over several days has also been seen in other studies. In one study,¹⁶ patients with recurrent glioblastoma multiforme tolerated absorbed doses of more than 300 Gy from [^{186}Re]-nanoliposomes delivered via convection-enhanced delivery.

Infusion volumes were well tolerated at all cohorts. With an infusion volume of approximately 4000 μL at cohort 7, the distribution volume was an average of 14.5 cm^3 and as high as 20 cm^3 (figure 2). This volume approximates that of the average tumour in diffuse intrinsic pontine glioma after radiation therapy, which has variously been reported to be 16–24 cm^3 (range 10–13–27–33)¹⁷ and 9–14 cm^3 .¹⁵ These estimates suggest that, in most patients, a single 4000 μL infusion could be distributed across the whole volume of the tumour. One caveat in our estimation of distribution volumes is that Vd estimation via T_2 -weighted signal change has not been validated. It is therefore possible that Vd measurements did not accurately estimate actual drug distribution. The mean Vd/Vi ratio in our study is, however, in close agreement with that reported from other studies in humans in which surrogate tracers were used in the brainstem.^{18–20} Surrogate tracers were intentionally omitted from this trial because uncertainty remains about their toxicity, such as the potential toxicity of Gd-based contrast agent deposition.²¹

A recommended phase 2 dose could not be established. For cytotoxic agents, the maximum tolerated dose is often regarded as synonymous of the recommended phase 2 dose. Because [^{124}I]-8H9 is a molecularly targeted agent, the traditional assumption that the highest tolerated dose is also the most efficacious might not apply. Although an infusion volume of 4000 μL produced a volume of distribution that approximated the average tumour volume after radiation therapy, it is not known whether larger infusion volumes could produce better tumour coverage or better therapeutic effects. Also unknown is whether larger doses of activity would be tolerated and could produce better therapeutic effects.

To our knowledge, this is the first study in humans to deliver an agent in a theranostic fashion for both brain cancer therapy and non-invasive dosimetry of the lesion and whole body. We provide in-human evidence of the ability of convection-enhanced delivery to efficiently deliver drugs into a target brain lesion with minimal systemic exposure. Our results also provide evidence that the radioisotope was retained in the lesion for more than 8 days.

Although cross-study comparisons should be made with caution, and this trial was not powered to assess overall survival, the patients in this study had a median overall survival that compares favourably with that of patients from most contemporary clinical studies.¹² Admittedly, our entry criteria could have introduced selection bias resulting in better

survival, as they eliminated patients with progressive disease or lower performance status, potentially leading to better survival results. The use of overall survival to monitor clinical benefit might have also been complicated by the fact that many patients were subsequently treated with various therapeutic strategies (ie, repeat radiation therapy) after exiting the trial. Event-free survival or progression-free survival might be more useful for monitoring clinical benefit, but the lack of a standardised definition of the event and inconsistencies in reporting also create limitations. Patients exiting our trial often received subsequent treatments before progression occurred. Nevertheless, the current results encouraged us to continue enrolling an expanded phase 1 cohort and to integrate this information into the design of a phase 2 trial, aiming to optimise drug distribution, tumour coverage, dosimetry, and scheduling.

Among the limitations of this study is the absence of diagnostic confirmation through tissue sampling. Erroneous diagnoses cannot be excluded because biopsies were not mandated for study entry. The criteria for study entry in this trial reflect those used for most contemporary cooperative group studies of diffuse intrinsic pontine glioma. Although stereotactic biopsy has been shown to be safe in children with diffuse intrinsic pontine glioma,^{22–24} transient or permanent morbidity associated with this procedure can reach 4%. We therefore decided that concomitant biopsy could complicate adverse event attribution, and decided not to perform it as part of this trial. Additionally, drug distribution has been shown to be negatively affected by adjoining cannula paths.²⁰

A legitimate concern related to the strategy of direct drug delivery is evidence that diffuse intrinsic pontine glioma can disseminate.^{25–27} It is possible that convection-enhanced delivery-based therapy, if used early enough in the disease course, could impart a survival benefit with local control. If regional control can be demonstrated with convection-enhanced delivery-based therapy, combinatorial approaches would be logical extensions of this strategy for future studies.

While the dual imaging and therapeutic capabilities of [¹²⁴I]-8H9 provided a way to use dosimetry to validate the principles of convection-enhanced delivery, a wide range of therapeutics could be delivered with convection-enhanced delivery in the treatment of diffuse intrinsic pontine glioma. Several studies^{28–30} have showed substantial genetic and epigenetic alterations in diffuse intrinsic pontine glioma, some of which are targetable with available therapeutic agents. These agents are known to have poor CNS penetration when delivered systemically, and thus convection-enhanced delivery might serve as an appealing delivery option for these agents.

The expression of B7-H3, the target of 8H9, is associated with poor prognosis in various tumours,^{31–33} and we previously reported variable expression patterns of B7-H3 between patients.⁸ Consequently, we are currently profiling B7-H3 expression from all available patients to correlate it with treatment response, in an attempt to establish whether expression patterns of B7-H3 could be a predictor of therapeutic benefit.

In conclusion, convection-enhanced delivery of [¹²⁴I]- 8H9 into the brainstems of patients with diffuse intrinsic pontine glioma was safe with our defined technique and parameters. Serious adverse events that might be related to the procedure were infrequent. Convection-

enhanced delivery-based therapeutic platforms warrant further development for the treatment of patients with diffuse intrinsic pontine glioma.

Supplementary Material

Refer to Web version on PubMed Central for supplementary material.

Acknowledgments

This study was supported in part by grant P30CA008748 from the National Institutes of Health, grants from the Dana Foundation Neuroimmunology Program, The Cure Starts Now, Solving Kids' Cancer, The Lyla Nsouli Foundation for Children's Brain Cancer Research, and Cookies for Kids' Cancer; contributions and donations from The Cristian Rivera Foundation, Battle for a Cure, Cole Foundation, Meryl & Charles Witmer Charitable Foundation, and Tuesdays with Mitch Charitable Foundation; and intramural funding from MSKCC (Pediatric Neurosurgery Fund, Center for Experimental Therapeutics grant, Fred's Team, and Perry's Promise). We thank the patients and their families who participated in the trial. We thank Joseph Olechnowicz of Pediatrics, MSKCC for assistance with select illustrations. We also thank the following organisations and programmes for past research support that made this study possible: The Alex's Lemonade Stand Foundation Pediatric Oncology Student Training Program, Humans of New York, The Ian's Friends Foundation, The Matthew Larson Foundation, The McKenna Claire Foundation, The Olivia Bocuzzi Foundation, Randi and Larry Cohen Family Foundation, The Children's Brain Tumor Family Foundation, The Pediatric Brain Tumor Foundation, and The St Baldrick's Foundation.

References

1. Hargrave D, Bartels U, Bouffet E. Diffuse brainstem glioma in children: critical review of clinical trials. *Lancet Oncol* 2006; 7: 241–48. [PubMed: 16510333]
2. Jansen MH, van Vuurden DG, Vandertop WP, Kaspers GJ. Diffuse intrinsic pontine gliomas: a systematic update on clinical trials and biology. *Cancer Treat Rev* 2012; 38: 27–35. [PubMed: 21764221]
3. Poussaint TY, Kocak M, Vajapeyam S, et al. MRI as a central component of clinical trials analysis in brainstem glioma: a report from the Pediatric Brain Tumor Consortium (PBTC). *Neuro Oncol* 2011; 13: 417–27 [PubMed: 21297126]
4. Bobo RH, Laske DW, Akbasak A, Morrison PF, Dedrick RL, Oldfield EH. Convection-enhanced delivery of macromolecules in the brain. *Proc Natl Acad Sci USA* 1994; 91: 2076–80. [PubMed: 8134351]
5. Zhou Z, Singh R, Souweidane MM. Convection-enhanced delivery for diffuse intrinsic pontine glioma treatment. *Curr Neuropharmacol* 2017; 15: 116–28. [PubMed: 27306036]
6. Xu H, Cheung IY, Guo HF, Cheung NK. MicroRNA miR-29 modulates expression of immunoinhibitory molecule B7-H3: potential implications for immune based therapy of human solid tumors. *Cancer Res* 2009; 69: 6275–81. [PubMed: 19584290]
7. Modak S, Kramer K, Gultekin SH, Guo HF, Cheung NK. Monoclonal antibody 8H9 targets a novel cell surface antigen expressed by a wide spectrum of human solid tumors. *Cancer Res* 2001; 61: 4048–54. [PubMed: 11358824]
8. Zhou Z, Luther N, Ibrahim GM, et al. B7-H3, a potential therapeutic target, is expressed in diffuse intrinsic pontine glioma. *J Neurooncol* 2013; 111: 257–64. [PubMed: 23232807]
9. Pagani M, Stone-Elander S, Larsson SA. Alternative positron emission tomography with non-conventional positron emitters: effects of their physical properties on image quality and potential clinical applications. *Eur J Nucl Med* 1997; 24: 1301–27 [PubMed: 9323273]
10. Modak S, Guo HF, Humm JL, Smith-Jones PM, Larson SM, Cheung NK. Radioimmunotargeting of human rhabdomyosarcoma using monoclonal antibody 8H9. *Cancer Biother Radiopharm* 2005; 20: 534–46. [PubMed: 16248769]
11. Storer BE. Design and analysis of phase I clinical trials. *Biometrics* 1989; 45: 925–37. [PubMed: 2790129]

12. Stabin MG, Sparks RB, Crowe E. OLINDA/EXM: the second-generation personal computer software for internal dose assessment in nuclear medicine. *J Nucl Med* 2005; 46: 1023–27. [PubMed: 15937315]
13. Brookmeyer R, Crowley J. A confidence interval for the median survival time. *Biometrics* 1982; 38:29–41.
14. Greenwood M A report on the natural duration of cancer Ministry of Health reports on public health and medical subjects. London: Her Majesty's Stationery Office, 1926.
15. Singh R, Zhou Z, Tisnado J, et al. A novel magnetic resonance imaging segmentation technique for determining diffuse intrinsic pontine glioma tumor volume. *J Neurosurg Pediatr* 2016; 18: 565–72. [PubMed: 27391980]
16. Bao A, Phillips W, Brenner A, et al. First-in-human study of ¹⁸⁶Re-nanoliposomes (186RNL) delivered intra-tumorally by convection-enhanced delivery for treatment of recurrent glioblastoma: Safety, image biodistribution, and radiation dosimetry. *J Nucl Med* 2017; 58 (suppl 1): abstr 599.
17. Sedlacik J, Winchell A, Kocak M, Loeffler RB, Broniscer A, Hillenbrand CM. MR imaging assessment of tumor perfusion and 3D segmented volume at baseline, during treatment, and at tumor progression in children with newly diagnosed diffuse intrinsic pontine glioma. *AJNR Am J Neuroradiol* 2013; 34: 1450–55. [PubMed: 23436052]
18. Voges J, Reszka R, Gossmann A, et al. Imaging-guided convection-enhanced delivery and gene therapy of glioblastoma. *Ann Neurol* 2003; 54: 479–87 [PubMed: 14520660]
19. Lonser RR, Warren KE, Butman JA, et al. Real-time image-guided direct convective perfusion of intrinsic brainstem lesions. Technical note. *J Neurosurg* 2007; 107: 190–97 [PubMed: 17639894]
20. Chittiboina P, Heiss JD, Warren KE, Lonser RR. Magnetic resonance imaging properties of convective delivery in diffuse intrinsic pontine gliomas. *J Neurosurg Pediatr* 2014; 13: 276–82. [PubMed: 24410126]
21. Olchoway C, Cebulski K, Lasecki M, et al. The presence of the gadolinium-based contrast agent depositions in the brain and symptoms of gadolinium neurotoxicity—a systematic review. *PLoS One* 2017; 12: e0171704.
22. Giese H, Hoffmann KT, Winkelmann A, Stockhammer F, Jallo GI, Thomale UW. Precision of navigated stereotactic probe implantation into the brainstem. *J Neurosurg Pediatr* 2010; 5: 350–59. [PubMed: 20367339]
23. Pincus DW, Richter EO, Yachnis AT, Bennett J, Bhatti MT, Smith A. Brainstem stereotactic biopsy sampling in children. *J Neurosurg* 2006; 104 (suppl 2): 108–14. [PubMed: 16506498]
24. Roujeau T, Machado G, Garnett MR, et al. Stereotactic biopsy of diffuse pontine lesions in children. *J Neurosurg* 2007; 107 (suppl 1): 1–4.
25. Wagner S, Benesch M, Berthold F, et al. Secondary dissemination in children with high-grade malignant gliomas and diffuse intrinsic pontine gliomas. *Br J Cancer* 2006; 95: 991–97 [PubMed: 17047647]
26. Sethi R, Allen J, Donahue B, et al. Prospective neuraxis MRI surveillance reveals a high risk of leptomeningeal dissemination in diffuse intrinsic pontine glioma. *J Neurooncol* 2011; 102: 121–27 [PubMed: 20623246]
27. Buczkowicz P, Bartels U, Bouffet E, Becher O, Hawkins C. Histopathological spectrum of paediatric diffuse intrinsic pontine glioma: diagnostic and therapeutic implications. *Acta Neuropathol* 2014; 128: 573–81. [PubMed: 25047029]
28. Zarghooni M, Bartels U, Lee E, et al. Whole-genome profiling of pediatric diffuse intrinsic pontine gliomas highlights platelet-derived growth factor receptor alpha and poly (ADP-ribose) polymerase as potential therapeutic targets. *J Clin Oncol* 2010; 28: 1337–44. [PubMed: 20142589]
29. Wu G, Broniscer A, McEachron TA, et al. Somatic histone H3 alterations in pediatric diffuse intrinsic pontine gliomas and non-brainstem glioblastomas. *Nat Genet* 2012; 44: 251–53. [PubMed: 22286216]
30. Lewis PW, Muller MM, Koletsky MS, et al. Inhibition of PRC2 activity by a gain-of-function H3 mutation found in pediatric glioblastoma. *Science* 2013; 340: 857–61. [PubMed: 23539183]
31. Zang X, Sullivan PS, Soslow RA, et al. Tumor associated endothelial expression of B7-H3 predicts survival in ovarian carcinomas. *Mod Pathol* 2010; 23: 1104–12. [PubMed: 20495537]

32. Zang X, Thompson RH, Al-Ahmadie HA, et al. B7-H3 and B7x are highly expressed in human prostate cancer and associated with disease spread and poor outcome. *Proc Natl Acad Sci USA* 2007; 104: 19458–63. [PubMed: 18042703]
33. Crispen PL, Sheinin Y, Roth TJ, et al. Tumor cell and tumor vasculature expression of B7-H3 predict survival in clear cell renal cell carcinoma. *Clin Cancer Res* 2008; 14: 5150–57 [PubMed: 18694993]

Author Manuscript

Author Manuscript

Author Manuscript

Author Manuscript

Research in context

Evidence before this study

We searched PubMed from March 15, 1994, up to Jan 31, 2018, with the terms “convection-enhanced delivery”, “diffuse intrinsic pontine glioma”, “brainstem”, “brainstem glioma”, and “clinical trials” for articles published in English. Children with diffuse intrinsic pontine glioma treated with radiation therapy, which is the standard of care, have a median overall survival of less than 1 year. To date, no therapeutic option offers a legitimate overall survival advantage over radiation therapy. Direct drug delivery by way of convection-enhanced delivery has been hypothesised as an appealing therapeutic strategy for patients with diffuse intrinsic pontine glioma; however, early clinical experience with single case reports has been highly varied, precluding the drawing of meaningful conclusions.

Added value of this study

To our knowledge, this phase 1 study is the first dose-escalation study to investigate the use of convection-enhanced delivery in patients with diffuse intrinsic pontine glioma. It is also the first-in-human study to directly deliver a radiolabelled antibody in a theranostic fashion for both dosimetry and brain cancer therapy. We report favourable safety profiles for both the surgical procedure and the therapeutic agent. We were also able to quantitate the absorbed dose of radiation in the tumour and other organs with PET imaging.

Implications of all the available evidence

These findings suggest that convection-enhanced delivery in the brainstem is clinically feasible and safe within defined parameters. Using PET-based dosimetry, we show evidence of high intralesional doses with negligible systemic exposure, validating the fundamental principle of convection-enhanced delivery. These results might serve as a foundation on which to design studies of convection-enhanced delivery-based therapies in the brainstem

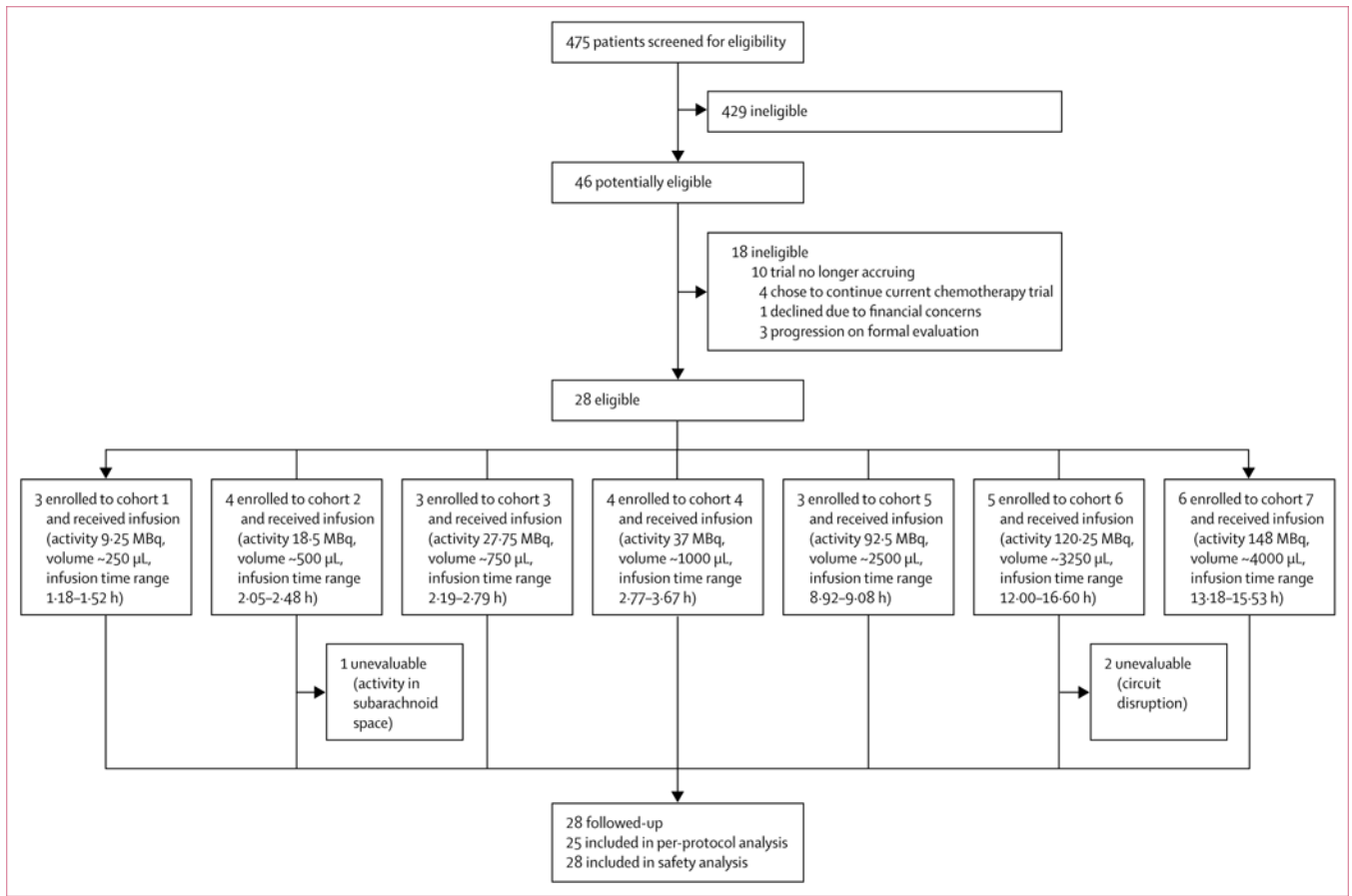


Figure 1: Trial profile

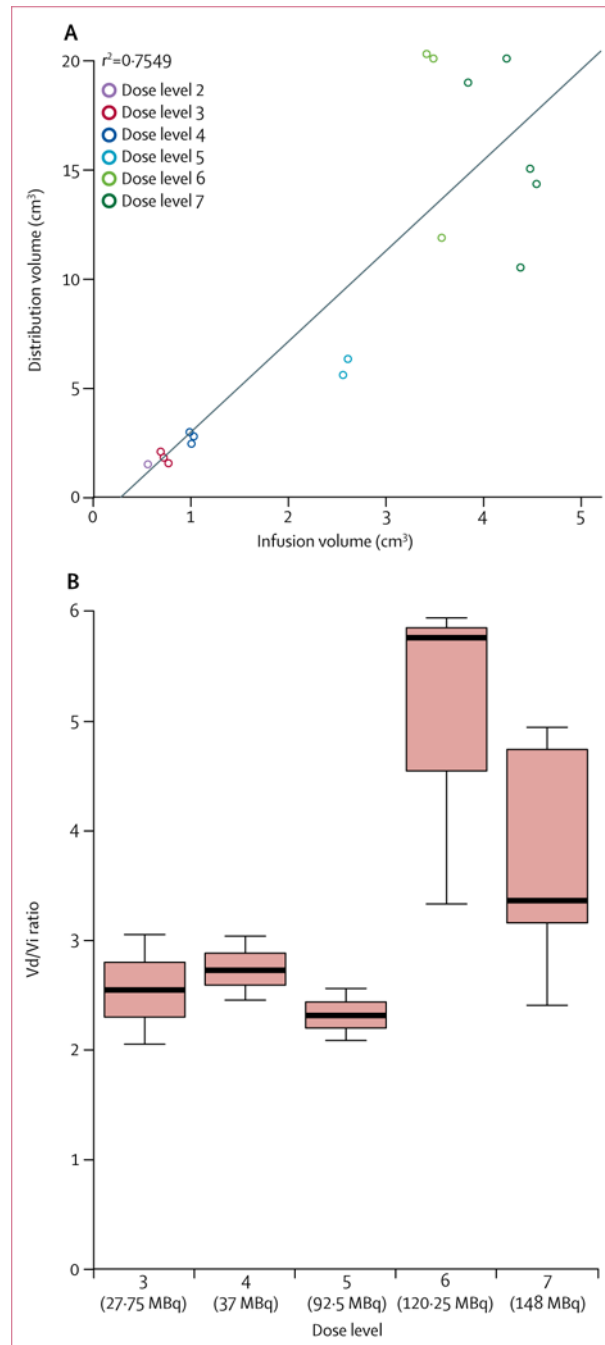


Figure 2: Relationships between distribution volume and infusion volume

(A) Relationship between Vd and Vi based on total infusion volumes for 17 patients with distribution data. Each data point represents one patient. Distribution volumes were determined from the first set of T2-weighted images acquired at infusion completion. (B) Vd/Vi ratio by dose level. No patients in dose level 1 and only one patient in dose level 2 were scanned for Vd determination. The boxplot is in Tukey convention (ie, maximum whiskers being $1.5 \times \text{IQR}$). Vd=volume distribution. Vi=infusion volume.

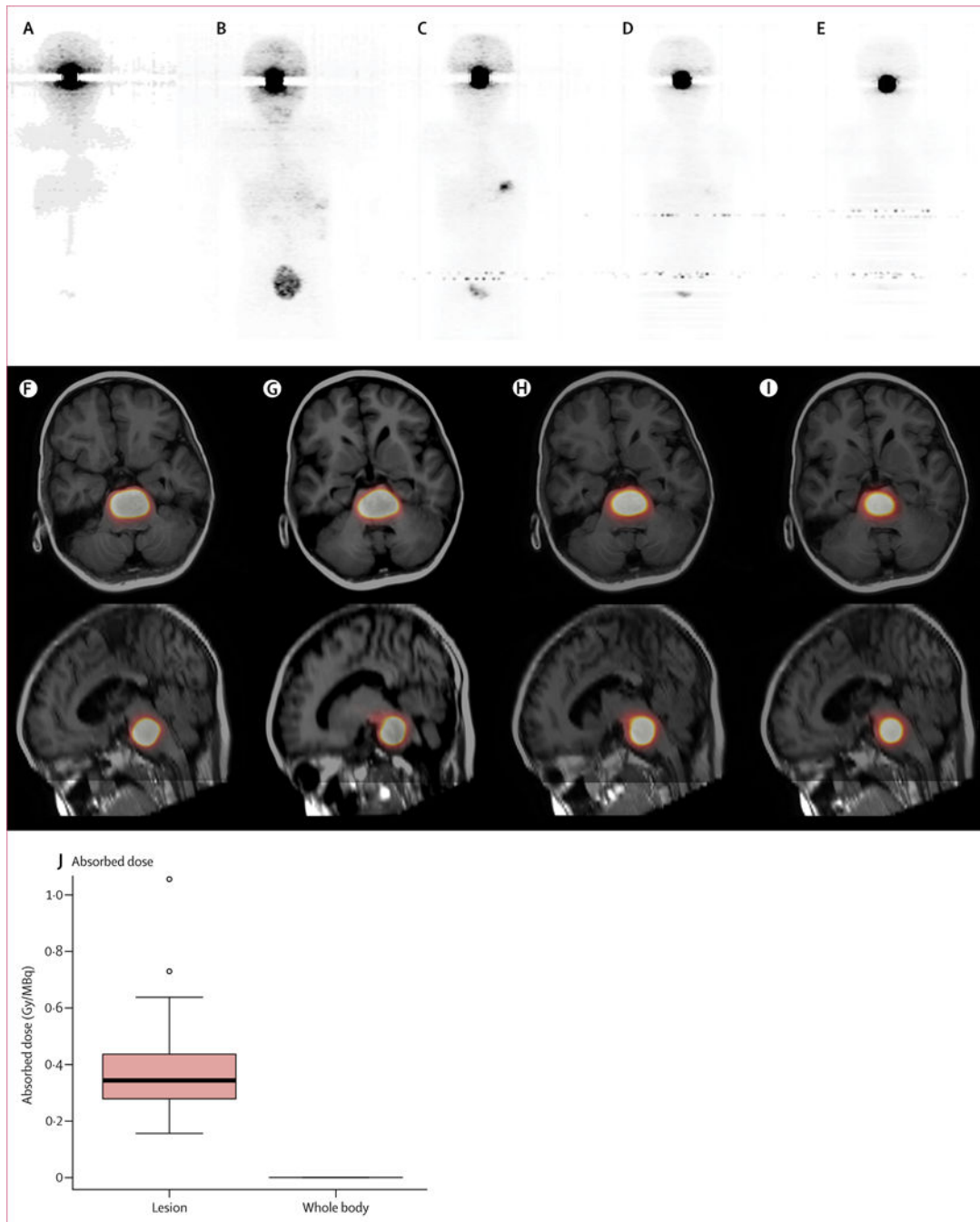


Figure 3: Delivery of ^{124}I -8H9 to the lesion on PET scans

(A-E) Whole-body scans from a representative patient showing high concentrations of ^{124}I in the brainstem. (A) 2 h after the completion of infusion, delivered activity was seen in the brainstem. (B) 48 h after completion of infusion. Predominant retention was shown in the brainstem infusion site, with a very small amount of activity in the blood pool and liver; excreted activity was seen in the urinary bladder. (C) 4 days after completion of infusion. Activity was still mainly notable in the brainstem, whereas activity in the bladder decreased compared with the 48-h scan; focal uptake in left upper quadrant of the abdomen represents

free iodide in stomach. (D) 6 days after completion of infusion. Activity in the brainstem persisted while activity in the remainder of the body, including the bladder, decreased. (E) 8 days after completion of infusion. Activity in the rest of the body was low, whereas activity in the brainstem was still prominently visible. (F-I) Brain PET fused images from a representative patient on cohort 7 (148 MBq, 4000 μ L) showing the delivery and retention of [124]-8H9. The upper sections are axial fused PET/MR images and the lower sections are sagittal fused PET/MR images. Fusion of the PET image onto the T1-weighted FLAIR images was achieved by co-registering MR images with CT images using bone markers in Hermes Hybrid Viewer 2.6G. The sagittal MR images were reconstructed from axial images. Images are from (F) 2 h, (G) 28 h, (H) 4 days, and (I) 8 days after infusion. (J) Radiation absorbed dose per MBq activity in the lesion and in the whole body. The boxplot is in Tukey convention (ie, maximum whiskers being $1.5 \times$ IQR). MR=magnetic resonance. FLAIR=fluid-attenuated inversion recovery.

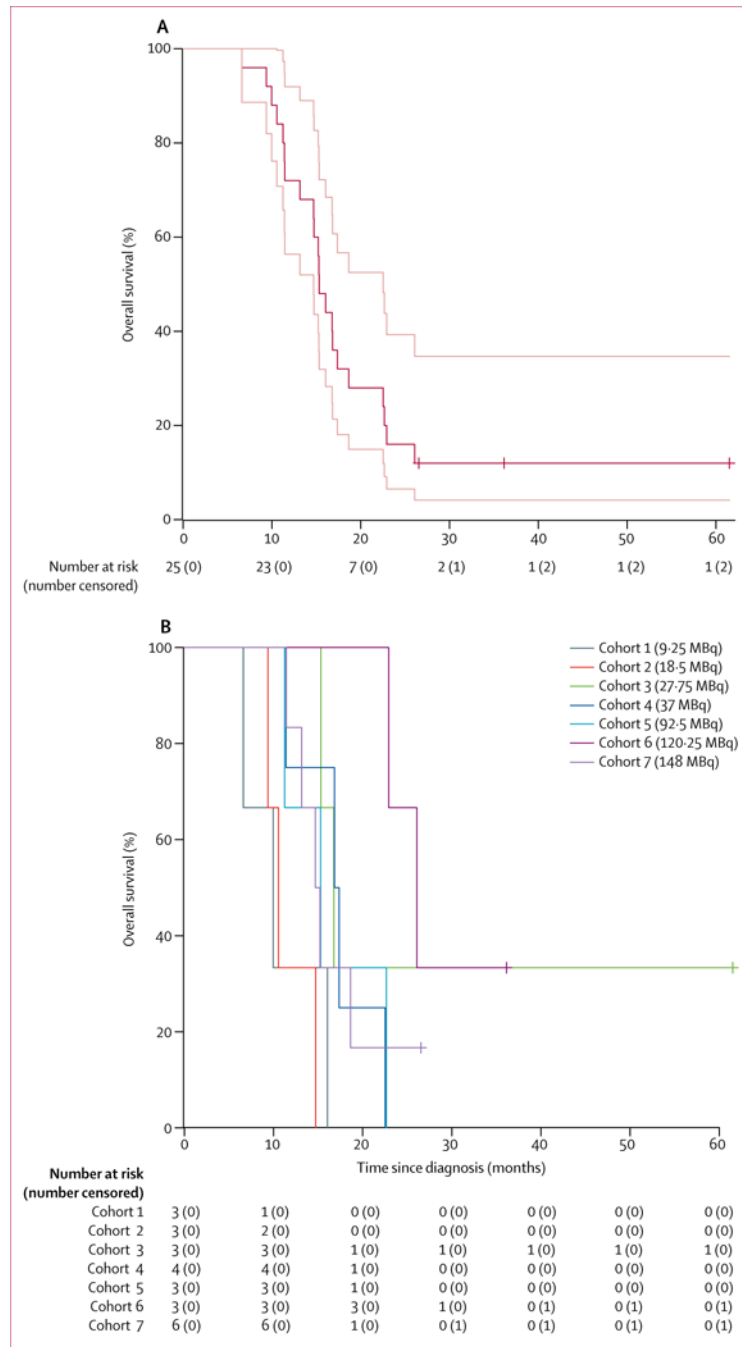


Figure 4: Overall survival

(A) Kaplan-Meier curve for the 25 evaluable patients and (B) by dose cohort. The pale lines in A show 95% CI for overall survival probability at each timepoint.

Table 1:

Baseline characteristics

	All patients (n=28)	Evaluable patients (n=25)
Age (years)		
Mean (SD)	8.0 (4.3)	8.2 (4.5)
Median (IQR)	6.7 (5.7–8.1)	6.5 (5.7–8.1)
Sex		
Male	17 (61%)	15 (60%)
Female	11 (39%)	10 (40%)
Race and ethnicity		
Caucasian	24 (86%)	21 (84%)
African	2 (7%)	2 (8%)
Asian	1 (4%)	1 (4%)
Native American	1 (4%)	1 (4%)
Hispanic	1 (4%)	1 (4%)
Non-Hispanic	27 (96%)	24 (96%)
Lansky/Karnofsky performance status		
Mean (SD)	90.7 (9.8)	90.4 (10.2)
Median (IQR)	90 (90–100)	90 (90–100)

Table 2:

All-cause adverse events

	Grade 1	Grade 2	Grade 3	Grade 4
Abducens palsy	3 (11%)	0	0	0
Agitation	2 (7%)	2 (7%)	0	0
Alanine aminotransferase increase	9 (32%)	0	0	0
Anaemia	3 (11%)	6 (21%)	0	0
Ankle clonus	3 (11%)	0	0	0
Anxiety	2 (7%)	2 (7%)	0	0
Activated partial thromboplastin time prolonged	3 (11%)	3 (11%)	1 (4%)	0
Aspartate aminotransferase increase	5 (18%)	2 (7%)	0	0
Ataxia	7 (25%)	0	1 (4%)	0
Cough	3 (11%)	0	0	0
Decreased rapid alternating movements	3 (11%)	0	0	0
Diplopia	6 (21%)	1 (4%)	0	0
Dysarthria	3 (11%)	0	1 (4%)	0
Dysmetria	5 (18%)	0	0	0
Dysphagia	2 (7%)	1 (4%)	0	0
Facial palsy	9 (32%)	1 (4%)	0	0
Fatigue	3 (11%)	0	0	0
Gait disturbance	4 (14%)	1 (4%)	0	0
Headache	8 (29%)	6 (21%)	0	0
Haemoglobin increased	5 (18%)	0	0	0
Hyperglycaemia	17 (61%)	10 (36%)	0	0
Hypernatraemia	6 (21%)	0	0	0
Hypertension	3 (11%)	2 (7%)	0	0
Hypoalbuminaemia	17 (61%)	0	0	0
Hypocalcaemia	4 (14%)	0	2 (7%)	0
Hypokalaemia	4 (14%)	0	3 (11%)	0
International normalised ratio increased	10 (36%)	0	0	0
Lymphocyte count decreased	5 (18%)	9 (32%)	10 (36%)	0
Muscle weakness, left-sided	4 (14%)	1 (4%)	1 (4%)	0
Muscle weakness, right-sided	3 (11%)	1 (4%)	2 (7%)	0
Nasal congestion	5 (18%)	1 (4%)	0	0
Neutrophil count decreased	7 (25%)	8 (29%)	0	0
Nystagmus	3 (11%)	0	0	0
Pain	6 (21%)	3 (11%)	0	0
Paraesthesia	3 (11%)	0	0	0
Platelet count decreased	7 (25%)	0	0	0
Rash, maculo-papular	2 (7%)	1 (4%)	0	0
Respiratory failure	0	0	0	1 (4%)
Skin infection	1 (4%)	0	1 (4%)	0

	Grade 1	Grade 2	Grade 3	Grade 4
Vomiting	3 (11%)	2 (7%)	0	0
White blood cells decreased	13 (46%)	6 (21%)	0	0

Grade 1 or 2 adverse events occurring in at least 10% of patients and all grade 3 and 4 events are reported. Adverse events are reported for all 28 treated patients. No treatment-related deaths occurred.

Author Manuscript

Author Manuscript

Author Manuscript

Author Manuscript